

RESONANCE PRODUCTION IN $\gamma\gamma$ REACTIONS

J.E. Olsson

D E S Y, Hamburg, West Germany

Abstract

Experimental results on the exclusive production of resonances in $\gamma\gamma$ collisions are reviewed. These include new measurements of the radiative widths of the pseudoscalar (η, η') and the tensor mesons (f, A_2, f'). A comparison of these results with SU(3) is made. Upper limits for other states than f in $\gamma\gamma \rightarrow \pi\pi$ are given. The searches for $\gamma\gamma$ production of the states ω and θ as well as η_c are presented and upper limits are given. Finally a limit is given for the rare decay $f \rightarrow \pi^+ \pi^- 2\pi^0$.

This review covers the recent results in single resonance production in $\gamma\gamma$ collisions. Reactions which involve double resonance production are dealt with in the talk by H. Kolanoski in these proceedings.

Resonance production in $\gamma\gamma$ collisions was first studied by using the Primakoff effect^(1,2); with a photon beam, resonances (π^0, η) were produced in the Coulomb field of nuclei. Today however, the main research is carried out at e^+e^- storage rings.

The basic diagram is shown below :

$$e^+e^- \rightarrow e^+e^-R \quad (1)$$

A characteristic feature of this diagram is the dominating low Q^2 of the emitted photons and the scattering of the electrons at small angles. The produced system R is boosted along the beam direction and its decay products are the only particles detected in the event, since the outgoing electrons are normally not seen (notag). The overall transverse momentum p_t of the system R is balanced with respect to the beam and this also constitutes an important criterium for the selection of exclusive final states in the experimental analysis. Furthermore, the C-parity of the resonances is C = +1 and the spin is different from 1, since the photons are almost real⁽³⁾.

The cross section for reaction (1) is given by

$$\sigma(e^+e^- \rightarrow e^+e^-R) = \int \sigma_{\gamma\gamma \rightarrow R}(s) L_{\gamma\gamma}(z) dz \quad (2)$$

Here s is the squared CM energy of the two photons and $\sigma_{\gamma\gamma}$ is the cross section for $\gamma\gamma \rightarrow R$. The density $L_{\gamma\gamma}$ is the luminosity function⁽⁴⁾ for the two photons and the variable $z = \sqrt{s}/2E_b$, with E_b the electron beam energy. The cross section $\sigma_{\gamma\gamma}$ is given by the Breit-Wigner formula

$$\sigma_{\gamma\gamma \rightarrow R} = 8\pi(2J+1) \Gamma_{R\gamma\gamma} \frac{\Gamma_R}{(m_R^2 - s)^2 + m_R^2 \Gamma_R^2} \quad (3)$$

where $2J+1$ is a spin factor, $\Gamma_{R\gamma\gamma}$ is the decay width into two photons and Γ_R is the full width of R. For a narrow resonance, $\Gamma_R/m_R \ll 1$ and the Breit-Wigner can be replaced by a δ -function, so that

$$\sigma(e^+e^- \rightarrow e^+e^-R) = \frac{8\pi^2 \Gamma_{R\gamma\gamma}}{m_R^2 4E_b} L_{\gamma\gamma} \left(\frac{m_R}{2E_b}\right) (2J+1) \quad (4)$$

In this expression the luminosity function $L_{\gamma\gamma}$ is still a complicated function. By

introducing the equivalent photon approximation⁽⁵⁾, (4) simplifies to⁽⁶⁾ :

$$\sigma(e^+e^- \rightarrow e^+e^-R) = \frac{16\alpha^2 \Gamma_{R\gamma\gamma}}{m_R^3} \left(\ln \frac{E_b}{m_e}\right)^2 f\left(\frac{m_R}{2E_b}\right) (2J+1) \quad (5)$$

The Low function $f(z)$ is given by $f(z) = (2+z^2) \ln(1/z) - (1-z^2)(3+z^2)$ and is a slowly varying function of resonance mass m_R and beam energy E_b . In (5) the dependence of the cross section $\sigma(e^+e^- \rightarrow e^+e^-R)$ on $\ln(E_b)$ as well as on the third power of the produced mass is clearly demonstrated.

This is all straightforward and a measurement of $\sigma(e^+e^- \rightarrow e^+e^-R)$ will give the corresponding value of the decay width of R into two photons, from (2), (4) or (5). However, there are several complications: firstly, the width $\Gamma_{R\gamma\gamma}$ refers to real photons and although the photons in reaction (1) have low Q^2 , they are virtual and the cross section has a Q^2 dependence which is not explicit in (3). This Q^2 dependence can be taken into account by introducing form factors for the photons, either with the standard ρ -pole, $1/(1+Q^2/m_\rho^2)^2$ or with a GVDM Ansatz⁽⁷⁾. A difference in the measured $\Gamma_{R\gamma\gamma}$ of 5-10% may result. Experiments rarely take this into account. Secondly, for decaying resonances care has to be taken to use correct matrix elements to describe the decays. Angular correlations among decay products and other dynamic effects may influence the overall detection efficiency and thereby the measurement of $\Gamma_{R\gamma\gamma}$. An example discussed at this conference is the decay $\eta' \rightarrow \gamma\eta^0$, which is a dipole transition⁽⁸⁾; $M^2 \sim q^2 k^2 m_{\eta\eta}^2 \sin^2 \theta$ |Breit-Wigner|², where q and k are the momenta of the pions and the photon and θ is the decay angle of the pions, all in the ρ rest system. In the recent measurements of $\Gamma_{\eta'\gamma\gamma}$ in the reaction $e^+e^- \rightarrow e^+e^-\eta'$ ⁽⁹⁻¹¹⁾, this matrix element seems not to be fully taken into account. A third complication is the small overall detection efficiency, typically a few % to a few %. This is caused by the boost along the beam axis, which together with the geometry of the detector tends to bring the final state particles out of the detector acceptance. The difficulties of triggering efficiently on an overall low energy final state at high energy e^+e^- storage rings also contributes, as well as the fact that the thresholds for detection of low energy particles, in particular photons, are in most detectors close to the typical energies of the involved particles.

All these considerations as well as other uncertainties combine to give relatively large systematic errors, typically 20% or more. Nevertheless the measurements are important, for several reasons. The main interest lies in the measurements of $\Gamma_{R\gamma\gamma}$. The absolute sizes of these widths are predicted in many models; in simple flavour SU(3) the quark content and mixing angle of the neutral mesons can be related to the relative sizes of the involved radiative widths. In some models glueballs mix with the standard $q\bar{q}$ mesons and again predictions are given about the radiative widths. Thus the measurements are needed to test such models. But there is also other

interest in reaction (1). With increasing integrated luminosities at the storage rings, the possibility to discover new $C = +1$ mesons should be kept in mind. $\gamma\gamma$ collisions form a clean source of meson production and bump hunting is a vivid part of two photon physics. And last but not least, the large integrated luminosities offer possibilities to study rare decay modes of well known resonances. As an example, $\sim 200\,000$ f mesons have so far been produced in each of the interaction regions at PETRA. Even with detection efficiencies in the 1% range, signals of rare decay modes may be detected and measured.

In the following, the present experimental data for the radiative widths of the pseudoscalars and the tensor mesons will be compared to the expectations from SU(3). It is therefore good to summarize the relevant formulae. In the meson nonet, the three neutral members are described by the following quark wave functions⁽¹²⁾ :

| | | |
|--|----------------|-------------------|
| $ 8,3\rangle = 1/\sqrt{2} (d\bar{d}-u\bar{u})$ | π^0, A_2^0 | isovector |
| $ 8,1\rangle = 1/\sqrt{6} (u\bar{u}+d\bar{d}-2s\bar{s})$ | η_8, f_8 | isoscalar octet |
| $ 1,1\rangle = 1/\sqrt{3} (u\bar{u}+d\bar{d}+s\bar{s})$ | η_1, f_1 | isoscalar singlet |

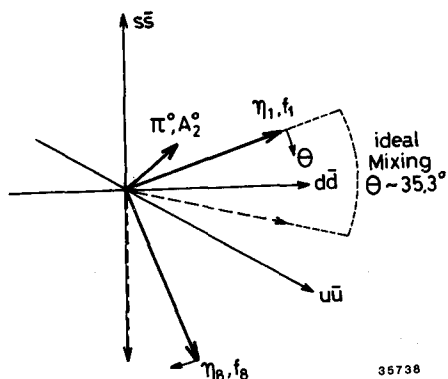


Fig. 1

Quark wave functions for the neutral members of the pseudoscalar and tensor meson nonets.

Fig. 1 shows these states in $u\bar{u}$, $d\bar{d}$ and $s\bar{s}$ space. The physical isoscalar particles are mixtures of the pure octet and singlet states¹:

$$\begin{aligned} \eta &= \cos \theta \eta_8 - \sin \theta \eta_1 & f' &= \cos \theta f_8 - \sin \theta f_1 \\ \eta' &= \sin \theta \eta_8 + \cos \theta \eta_1 & f &= \sin \theta f_8 + \cos \theta f_1 \end{aligned} \quad (6)$$

The mixing angle thus represents a rotation about the isovector axis. For a value of $\sim 35.3^\circ$, the so called ideal mixing is obtained, with pure $s\bar{s}$ and pure $u\bar{u}$, $d\bar{d}$ states. With some further assumptions (e.g. equality of the quark magnetic moments), the couplings of the states to two photons can be related⁽¹²⁾,

¹ In some textbooks, the states $|8,3\rangle = 1/\sqrt{2} (u\bar{u}-d\bar{d})$ and $|8,1\rangle = 1/\sqrt{6} (2s\bar{s}-u\bar{u}-d\bar{d})$ are used.

$$M_{\eta_0\gamma\gamma} = -\sqrt{\frac{1}{3}} M_{\pi^0\gamma\gamma} \quad M_{\eta_1\gamma\gamma} = -\sqrt{\frac{8}{3}} M_{\pi^0\gamma\gamma} \quad (7)$$

and one obtains the following relations between the corresponding radiative widths:

$$\begin{aligned} \Gamma_{\eta\gamma\gamma} &= \Gamma_{\pi^0\gamma\gamma} \left(\frac{m_\eta}{m_{\pi^0}}\right)^3 \frac{1}{3} (\sqrt{8} \sin \theta - \cos \theta)^2 \\ \Gamma_{\eta'\gamma\gamma} &= \Gamma_{\pi^0\gamma\gamma} \left(\frac{m_{\eta'}}{m_{\pi^0}}\right)^3 \frac{1}{3} (\sin \theta + \sqrt{8} \cos \theta)^2 \\ \Gamma_{\eta'\gamma\gamma} &= \Gamma_{\eta\gamma\gamma} \left(\frac{m_{\eta'}}{m_\eta}\right)^3 \left(\frac{\sin \theta + \sqrt{8} \cos \theta}{\sqrt{8} \sin \theta - \cos \theta}\right)^2 \end{aligned} \quad (8)$$

$$\begin{aligned} \Gamma_{f'\gamma\gamma} &= \Gamma_{A_2\gamma\gamma} \left(\frac{m_{f'}}{m_{A_2}}\right)^3 \frac{1}{3} (\sqrt{8} \sin \theta - \cos \theta)^2 \\ \Gamma_{f\gamma\gamma} &= \Gamma_{A_2\gamma\gamma} \left(\frac{m_f}{m_{A_2}}\right)^3 \frac{1}{3} (\sin \theta + \sqrt{8} \cos \theta)^2 \\ \Gamma_{f\gamma\gamma} &= \Gamma_{f'\gamma\gamma} \left(\frac{m_f}{m_{f'}}\right)^3 \left(\frac{\sin \theta + \sqrt{8} \cos \theta}{\sqrt{8} \sin \theta - \cos \theta}\right)^2 \end{aligned} \quad (9)$$

$$\frac{\Gamma_{A_2\gamma\gamma}}{\Gamma_{f\gamma\gamma}} = \left(\frac{m_{A_2}}{m_f}\right)^3 \frac{3}{(\sin \theta + \sqrt{8} \cos \theta)^3} \quad (10)$$

Here the mass powers are phase space factors. Thus the measured radiative widths give values for the mixing angles which can be compared with the mixing angle values obtained in studies of other reactions involving these particles.

When presenting the experimental situation of today, the results divide naturally into three parts. After starting with the pseudoscalars, the tensor mesons are presented and discussed and finally the remaining results can conveniently be grouped under the heading "upper limits". But let us begin with the neutral members of the pseudoscalar nonet. These are all well established mesons and the branching ratios into $\gamma\gamma$ are well known. The width of π^0 is known from measurements of the lifetime⁽¹³⁾ as well as from photoproduction experiments⁽¹⁴⁾. It is here worthwhile to mention that a new experiment (NA30)⁽¹⁴⁾ is under way at the CERN SPS, with the goal to measure τ_{π^0} to 1% precision (present accuracy 7%). The method consists essentially of

producing π^0 's in a gold foil via the proton beam and measuring the rate of conversion electrons behind a second foil; this rate depends on whether the pions decay before or after passing the second foil. Thus the rate of electrons as function of foil distance will allow a measurement of τ_{π^0} and thereby $\Gamma_{\pi^0\gamma\gamma}$, since the branching ratio $B(\pi^0 \rightarrow \gamma\gamma)$ is very well known, $0.98787 \pm 0.00030^{(16)}$. The main run for the experiment is scheduled for the autumn 1983.

Measurements of $\Gamma_{\pi^0\gamma\gamma}$ at e^+e^- storage rings have not yet been performed, mainly because of the problems of triggering and detecting such a low energy final state. For the same reasons, the measurement of $\Gamma_{\eta\gamma\gamma}$ is a difficult task. However, at this conference the Crystal Ball group now reports the first measurement of the process $e^+e^- \rightarrow e^+e^-\eta, \eta \rightarrow \gamma\gamma$, at SPEAR. For this purpose, a special "topology" trigger was installed for low energy neutral final states. Essentially, the ball is divided into two opposite hemispheres in several different ways and the trigger condition is given by a certain minimum energy in each of the two hemispheres. The main background in such a trigger mode comes from cosmic radiation, which however can be well rejected with a series of cuts, using chamber information, energy patterns in the crystals and the timing of the energy measurement. The $\gamma\gamma$ mass spectrum for exclusively two photons in the final state, after all cuts, is shown in Fig. 2a. A clear peak at the η mass is seen. However, η 's may also come from electroproduction off the residual gas in the vacuum pipe. To obtain information on this, data were also taken with separated beams and the corresponding mass spectrum is shown in Fig. 2b. Also here a peaking at the η mass is seen. Normalizing this spectrum to the colliding beam data in Fig. 2a and subtracting, the mass distribution in Fig. 3 is obtained. It is well

fitted by a Gaussian close to the η mass and the width agrees with the values from other η spectra in the Crystal Ball. The total integrated luminosity is only 2.7 pb^{-1} and this accounts for the low statistics; nevertheless, one cannot enough stress the beauty of this spectrum.

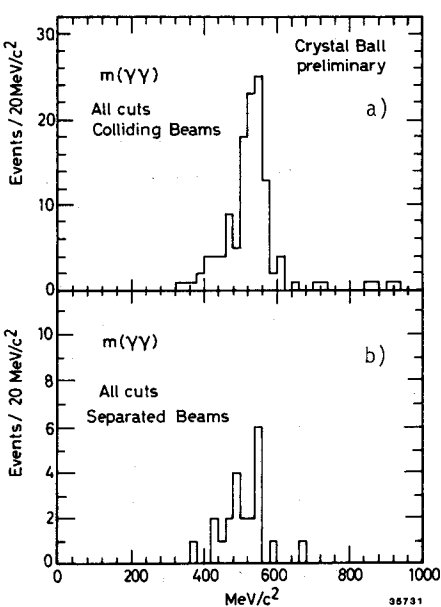


Fig. 2

- a) Mass spectrum of 2γ in events with exclusively 2γ in the final state. Data with colliding beams.
- b) Same, but data with separated beams. The normalization corresponds to about 37% of the data in a).

From these data, the group obtains the radiative width value,

$$\Gamma_{\eta\gamma\gamma} = 0.56 \pm 0.12 \text{ (stat.)} \pm 0.09 \text{ (syst.) keV} \quad \text{(preliminary)}$$

which is larger than the previous measurement of Browman et al. ⁽²⁾ at Cornell in 1974. This experiment used the Primakoff effect and obtained the value $\Gamma_{\eta\gamma\gamma} = 324 \pm 46$ keV. These are the only measurements available so far. They represent two different experimental techniques, each with its own kind of systematic error sources. Comparing them, one should remember that the first one still has a large statistical error, which hopefully can be improved in the future; and the Cornell group also measured $\Gamma_{\pi^0\gamma\gamma}$ ⁽¹⁾, in good agreement with measurements of τ_{π^0} ⁽¹³⁾.

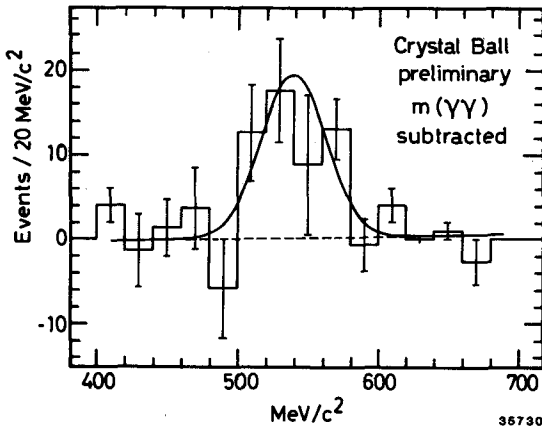


Fig. 3

Mass spectrum of 2γ in exclusive 2γ events. The beam gas background in Fig. 2b has been normalized and subtracted from the data in Fig. 2a. The curve is a gaussian fit.

The $\gamma\gamma$ width of the third pseudo-scalar, η' , has now been measured by several groups in e^+e^- collisions. After the first measurement by the MARK II

collaboration ⁽⁹⁾, also the CELLO ⁽¹⁰⁾ and JADE ⁽¹¹⁾ collaborations published measurements last year. Like the MARK II collaboration, both groups used the decay mode $\eta' \rightarrow \gamma\rho^0$ and the final state is $\pi^+\pi^-\gamma$ exclusive. The two $\pi^+\pi^-\gamma$ mass spectra from such events are shown in Figs. 4a and b, respectively. In both figures, events with the $\pi^+\pi^-$ mass in a ρ band are shown as hatched distributions. The second peak in Fig. 4a is due to the incompletely reconstructed decay $A_2 \rightarrow \rho^+\pi^+ \rightarrow \pi^+\pi^-\pi^0$, where a photon from an asymmetric π^0 -decay is lost. In Fig. 4b, events with $\pi^+\pi^-$ masses above 1 GeV/c² are excluded, which reduces the background in the A_2 region. For the width $\Gamma_{\eta'\gamma\gamma}$, the values $\Gamma_{\eta'\gamma\gamma} = 6.2 \pm 1.1$ (stat.) ± 0.8 (syst.) keV and $\Gamma_{\eta'\gamma\gamma} = 5.0 \pm 0.5 \pm 0.9$ keV were obtained, respectively.

At this conference a new, preliminary measurement by the TASSO collaboration is presented. Again, the decay mode $\eta' \rightarrow \gamma\rho^0$ is used; the mass spectrum of $\pi^+\pi^-\gamma$ is shown in Fig. 5 and exhibits a nice η' signal. The $\gamma\rho^0$ decay is shown by the shaded distribution with the $\pi^+\pi^-$ mass limited to the ρ^0 interval. The spectrum is in fact the sum of the two spectra obtained from the two different sets of shower counters used in TASSO to detect photons, liquid argon (LA) in top and bottom and lead-scintillator sandwich counters (SC) at the end of the lateral spectrometer arms. The data

comprise 75 pb^{-1} . The value of the radiative width,

$$\Gamma_{\eta' \gamma\gamma} = 4.1 \pm 0.4 \text{ (stat.)} \pm 1.5 \text{ (syst.) keV} \quad (\text{preliminary})$$

is the mean of the two values obtained from the LA and SC parts, both of which however are close to 4 keV. The large systematic error is mainly connected with the Monte Carlo simulation, which is still under study. A similar measurement is under way in the PLUTO collaboration⁽¹⁵⁾, but no value of $\Gamma_{\eta' \gamma\gamma}$ is available yet.

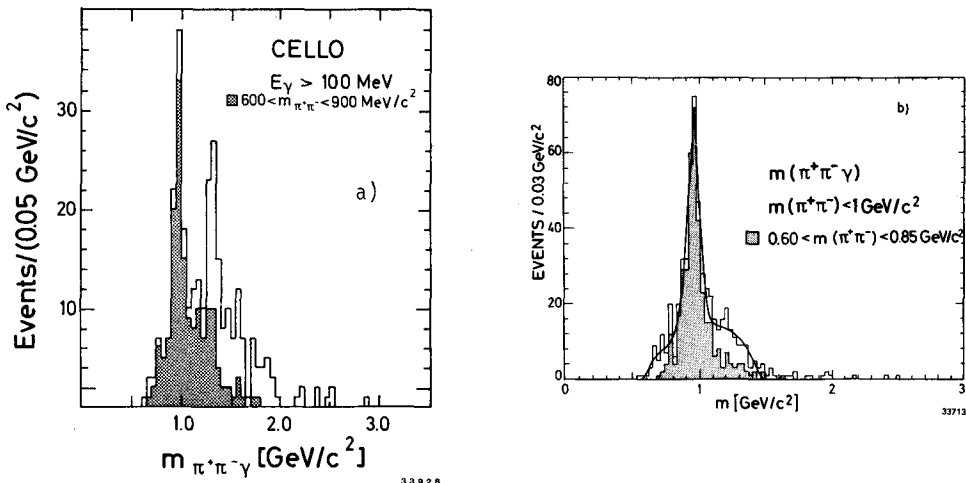


Fig. 4

Mass spectrum of the $\pi^+\pi^-\gamma$ system in exclusive $\pi^+\pi^-\gamma$ events. The shaded distributions correspond to events with the $\pi^+\pi^-$ mass in a ρ -band.

a) CELLO, data from 11 pb^{-1} . A cut, $p_t(\pi^+\pi^-\gamma) < 0.2 \text{ GeV}/c$, has been applied.
b) JADE, data from 36 pb^{-1} . A cut, $p_t(\pi^+\pi^-\gamma) < 0.6 \text{ GeV}/c$, has been applied.

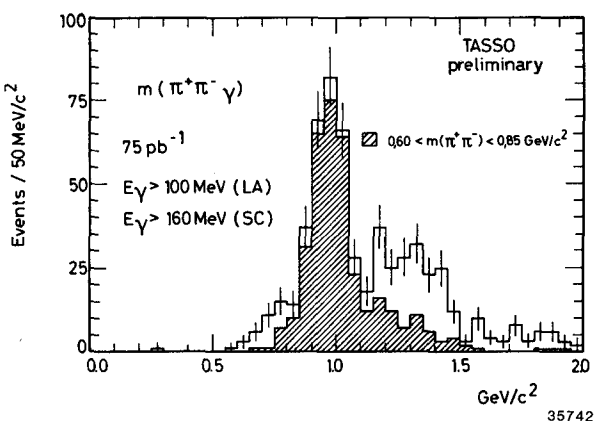


Fig. 5

Mass spectrum of $\pi^+\pi^-\gamma$, from events with exclusively two charged pions and one photon. The shaded distribution corresponds to events with the $\pi^+\pi^-$ mass in a ρ -band. A cut, $p_t(\pi^+\pi^-\gamma) < 0.1 \text{ GeV}/c$, has been applied.

The present situation of $\Gamma_{\eta\eta\eta}$ and $\Gamma_{\eta'\eta\eta}$ measurements is summarized in Table 1. The $\Gamma_{\eta\eta\eta}$ values agree well with the various predictions from fractionally charged quark models, 4-7 keV, while the large values, ~26 keV, from integrally charged quark models are clearly ruled out^(16,29). The mean value is 5.3 ± 0.6 keV. Taking the mean of only the e^+e^- measurements and using $B(\eta' \rightarrow \gamma\gamma) = 1.9 \pm 0.2\%$, the total width of η' is obtained, $\Gamma_{\eta'} = 276 \pm 45$ keV, which agrees very nicely with the missing mass measurement of Binnie et al.⁽¹⁷⁾, $\Gamma_{\eta'} = 280 \pm 100$ keV. It is also interesting to note (Budnev and Kaloshin⁽¹⁶⁾) that the measurement of the total width, which gives $\Gamma_{\eta'\eta\eta}$ by using $B(\eta' \rightarrow \gamma\gamma)$, together with the e^+e^- values give a measurement of the spin $J_{\eta'}$ of η' , since $\sigma(e^+e^- \rightarrow e^+e^-\eta')$ is proportional to $(2J_{\eta'} + 1)\Gamma_{\eta'\eta\eta}$.

Quark model predictions for $\Gamma_{\eta\eta\eta}$ range from 300 - 800 eV⁽¹⁶⁾. Here the distinction between integral and fractional charge quarks is not so marked, although the data in Table 1 favours the latter. The measurement of $\Gamma_{\eta'\eta\eta}$ is in fact one of the strongest experimental evidences for fractionally charged quarks.

We now compare the measured values of $\Gamma_{\eta\eta\eta}$ and $\Gamma_{\eta'\eta\eta}$ with the SU(3) relations (8). This is done in Figs. 6a and b. Fig. 6a shows the widths $\Gamma_{\eta'\eta\eta}$ and $\Gamma_{\eta\eta\eta}$ as functions of the mixing angle θ , with the width $\Gamma_{\pi^0\eta\eta}$ fixed at the Particle Data Group (PDG) value⁽¹⁸⁾, 7.85 eV. The mean value of $\Gamma_{\eta'\eta\eta}$ and the two measurements of $\Gamma_{\eta\eta\eta}$ from Crystal Ball and Cornell are also shown, together with the corresponding ranges in the mixing angle. One sees that the $\Gamma_{\eta'\eta\eta}$ value and the Crystal Ball value of $\Gamma_{\eta\eta\eta}$ cover the same range, $\theta \sim -18 \pm 5^\circ$, while the Cornell measurement gives $\theta \sim -7.5 \pm 2.5^\circ$.

In Fig. 6b $\Gamma_{\eta'\eta\eta}$ is shown as function of θ and of $\Gamma_{\eta\eta\eta}$; the bands from the two measurements of $\Gamma_{\eta\eta\eta}$ are indicated, together with the θ ranges. Here a small region of overlap in θ is present, which however would correspond to rather small values of $\Gamma_{\pi^0\eta\eta}$ (~7 eV). As comparison, one may note that the quadratic mass formula⁽¹⁸⁾ gives the value $\theta = -11.1 \pm 0.2^\circ$. Larger negative values, $\theta = -17$ to -20° were found in a QCD calculation⁽¹⁹⁾; $\theta = -16 \pm 2^\circ$ was found in a study of the reaction $\pi^-p \rightarrow \eta'n \rightarrow \gamma\gamma\eta$ ⁽²⁰⁾.

When making comparisons like this, one should remember that the relations (8) are based on naive and simplifying assumptions. The mixing situation in the pseudoscalar nonet is certainly much more complex and to clarify the large deviation from ideal mixing encountered in the pseudoscalar nonet is a longstanding and famous theoretical problem⁽²¹⁾. It is however clear that the measurement of the $\gamma\gamma$ widths is an important input to its eventual solution and that in particular better measurements of $\Gamma_{\eta\eta\eta}$ in e^+e^- storage rings are needed.

* * *

Table 1
Radiative Widths of Pseudoscalar Mesons

| Experiment | $\Gamma_{\eta\eta\gamma\gamma} \pm (\text{stat.}) \pm (\text{syst.}) \text{ keV}$ |
|--------------------------------|---|
| Browman et al. Crystal Ball | 0.324 ± 0.046 $0.56 \pm 0.12 \pm 0.09$ (prel.) |
| Weighted Mean : | $0.344 \pm 0.044 \text{ keV}$ |

| Experiment | $\Gamma_{\eta'\eta\gamma\gamma} \pm (\text{stat.}) \pm (\text{syst.}) \text{ keV}$ |
|--|---|
| Binnie et al. MARK II CELLO JADE TASSO | 5.4 ± 2.1 $5.8 \pm 1.1 \pm 1.2$ $6.2 \pm 1.1 \pm 0.8$ $5.0 \pm 0.5 \pm 0.9$ $4.1 \pm 0.4 \pm 1.5$ (prel.) |
| Weighted Mean : | $5.3 \pm 0.6 \text{ keV}$ |

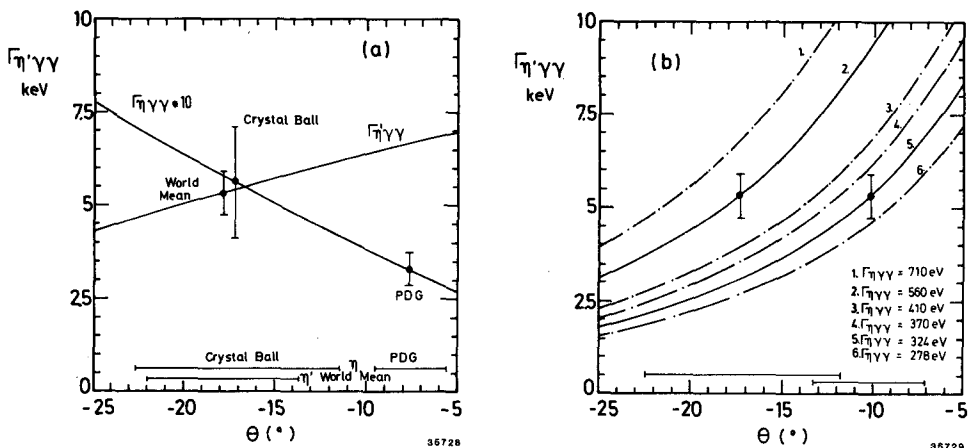


Fig. 6 a) $\Gamma_{\eta'\eta\gamma\gamma}$ and $\Gamma_{\eta\eta\gamma\gamma}$ as function of the mixing angle θ , with $\Gamma_{\eta\eta\gamma\gamma} = 7.85 \text{ eV}$. $\Gamma_{\eta\eta\gamma\gamma}$ is multiplied by 10. The measurements of $\Gamma_{\eta'\eta\gamma\gamma}$ and $\Gamma_{\eta\eta\gamma\gamma}$ are shown as data points. PDG stands for the measurement of $\Gamma_{\eta\eta\gamma\gamma}$ from Cornell. The corresponding ranges in θ are given by the errors.
b) $\Gamma_{\eta'\eta\gamma\gamma}$ as function of mixing angle θ and $\Gamma_{\eta\eta\gamma\gamma}$. The curves correspond to the two measurements of $\Gamma_{\eta\eta\gamma\gamma}$. The data point in each band is the mean value of $\Gamma_{\eta'\eta\gamma\gamma}$ from Table 1.

The two photon production of the tensor mesons has also received a lot of work in the last years. The $f(1270)$ meson has long posed a problem of measurement⁽²²⁻²⁴⁾ in the reaction $e^+e^- \rightarrow e^+e^-f$, $f \rightarrow \pi^+\pi^-$, since the resonance appears together with a sizeable continuum from the reaction $\gamma\gamma \rightarrow \pi^+\pi^-$ and shows a distortion in mass and width. An early explanation for this was given by the MARK II group⁽²³⁾, who showed that the data could be explained with an interference between a continuum Born amplitude and a d-wave Breit-Wigner. At this conference, the CELLO collaboration presents

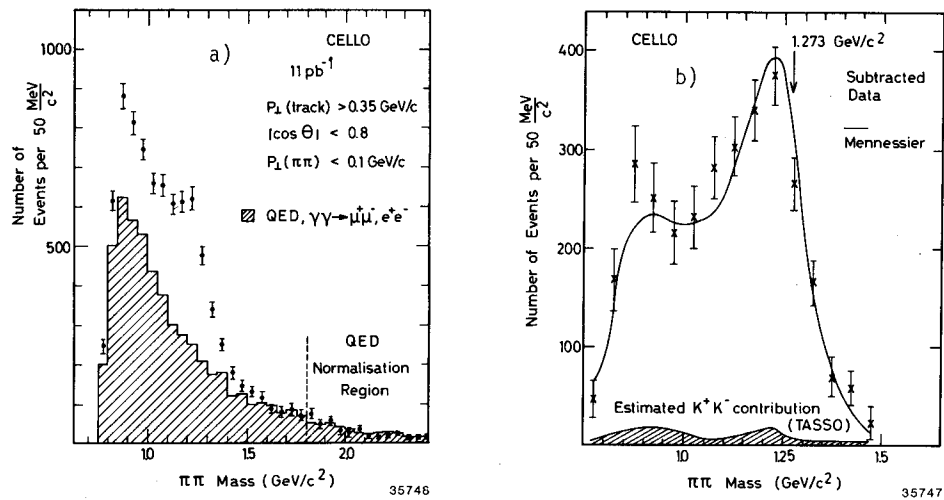


Fig. 7

a) $\pi^+\pi^-$ mass spectrum in exclusive two prong events. The hatched distribution shows the QED contribution.

b) The same data with the QED contribution subtracted. The hatched distribution shows the K^+K^- part. The curve is explained in the text.

a new analysis of this reaction. The mass spectrum of $\pi^+\pi^-$ from exclusive two prong events is shown in Fig. 7a. The data also contain events from the QED reactions $e^+e^- \rightarrow e^+e^-e^+e^-$ and $e^+e^- \rightarrow e^+e^-\mu^+\mu^-$. This contribution is calculated using the exact cross section⁽⁴⁾ and is shown in the hatched distribution in Fig. 7a. It has been normalized to the data for $\pi\pi$ masses above $1.8 \text{ GeV}/c^2$, since other studies⁽²⁵⁾ show that the hadronic contribution is small at high masses. The calculated absolute rate however agrees with the event rate in this mass region and also other distributions are in excellent agreement with the QED expectations.

After subtraction of the QED contribution the mass spectrum in Fig. 7b remains. It shows clearly the f resonance situated on a large $\pi\pi$ continuum and with a visibly displaced mass. To analyze this spectrum, the model of G. Mennessier⁽²⁶⁾ has been used. In this model, the Born amplitude is unitarized, i.e. strong interactions in the final state are included, with help of measured $\pi\pi$ and KK phase shifts and

inelasticities. The size of the K^+K^- contribution (misinterpreted as $\pi^+\pi^-$) is taken from the TASSO measurement⁽²⁷⁾. In the version of the model used here, there is only one free parameter, namely $\Gamma_{f\gamma\gamma}$. The standard values⁽¹⁸⁾ for f mass and full width are used as input in the calculations and pure helicity 2 is assumed for the f amplitude, in accordance with the result in Ref. 24 (dominance of helicity 2 was found in a study of the decay angular distribution of the reaction $\gamma\gamma \rightarrow f \rightarrow \pi^0\pi^0$). With this application of the Mennessier model the observed shift of the f mass of ~ 50 MeV/c² is again explained as due to interference between the Born term and the f resonance, constructive below and destructive above f. In the fit of the model to the data, shown in Fig. 7b, the following value for the radiative width is found,

$$\Gamma_{f\gamma\gamma} = 2.7 \pm 0.2 \text{ (stat.)} \pm 0.2 \text{ (syst.) keV} \quad \text{(preliminary).}$$

It is in good agreement with previous measurements⁽²²⁻²⁴⁾. It is however preliminary; the absolute normalization of the QED contribution (Fig. 7a) is still being studied.

The decay mode $f \rightarrow \pi^0\pi^0$ was first measured by the Crystal Ball group⁽²⁴⁾ at SPEAR and recently also by the JADE collaboration at PETRA. The JADE data are shown in Figs. 7 and 8. The final state is now 4 γ exclusive. The scatter plot in Fig. 8a of $\gamma\gamma$ mass vs. $\gamma\gamma$ mass (3 combinations per event) shows a strong signal of associated $\pi^0\pi^0$ production; the sum of the projections is shown in Fig. 8b. For the events in the $2\pi^0$ interval, the photon energies are now adjusted so that the final state is $2\pi^0$. The corresponding mass of $2\pi^0$ is shown in Fig. 9 and exhibits a clear f peak. The integrated luminosity is 32 pb^{-1} at 17.3 GeV beam energy. The radiative width of f, assuming pure helicity 2 in the production, is determined to be

$$\Gamma_{f\gamma\gamma} = 2.3 \pm 0.2 \text{ (stat.)} \pm 0.5 \text{ (syst.) keV} \quad \text{(preliminary).}$$

Apart from the f signal, only few events are present in the spectrum in Fig. 9. This was also found in the Crystal Ball analysis. The CELLO group has applied the Mennessier model also to this decay mode and finds that the model explains the Crystal Ball data well if the ω exchange term is suppressed, since its inclusion would lead to too high a level of $\pi^0\pi^0$ continuum. The level predicted by the final state rescattering process $\gamma\gamma \rightarrow \pi^+\pi^- \rightarrow \pi^0\pi^0$ agrees however. A small mass shift of f is also predicted, in agreement with the observed shift in the Crystal Ball analysis; the model does not, however, explain the large total f width, $\Gamma_f = 248 \pm 38$ MeV, observed in the same experiment. For the JADE data no values for the f mass and width in the $\pi^0\pi^0$ mass spectrum have been given yet.

It thus seems that interference between the $\gamma\gamma \rightarrow \pi^+\pi^-$ Born amplitude and the f resonance gives a satisfactory description of the $\pi^+\pi^-$ spectrum produced in $\gamma\gamma$ reactions. It should here be mentioned that also other explanations could be advanced, notably

Fig. 8

a) Scatterplot of $m(\gamma\gamma)$ vs. $m(\gamma\gamma)$ in exclusive 4γ events. All photon energies are > 90 MeV.

b) Sum of the projections of the scatterplot in a).

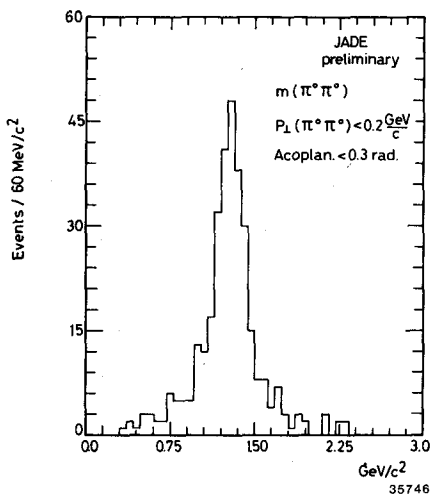
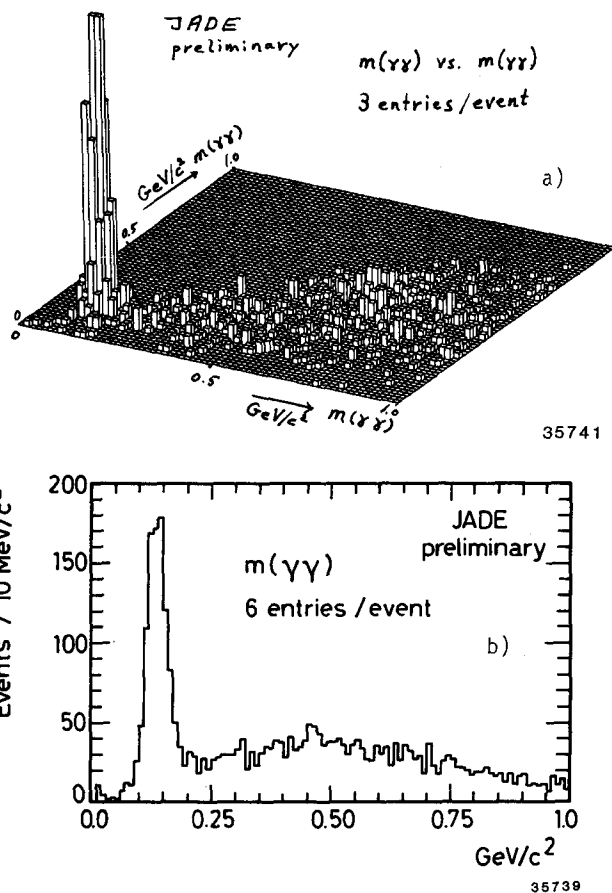


Fig. 9

Mass of $2\pi^0$, for events with two $m(\gamma\gamma)$ combinations in the π^0 band, $90-190$ MeV/c². The photon energies have been adjusted so that $m(\gamma\gamma) = m_{\pi^0}$.

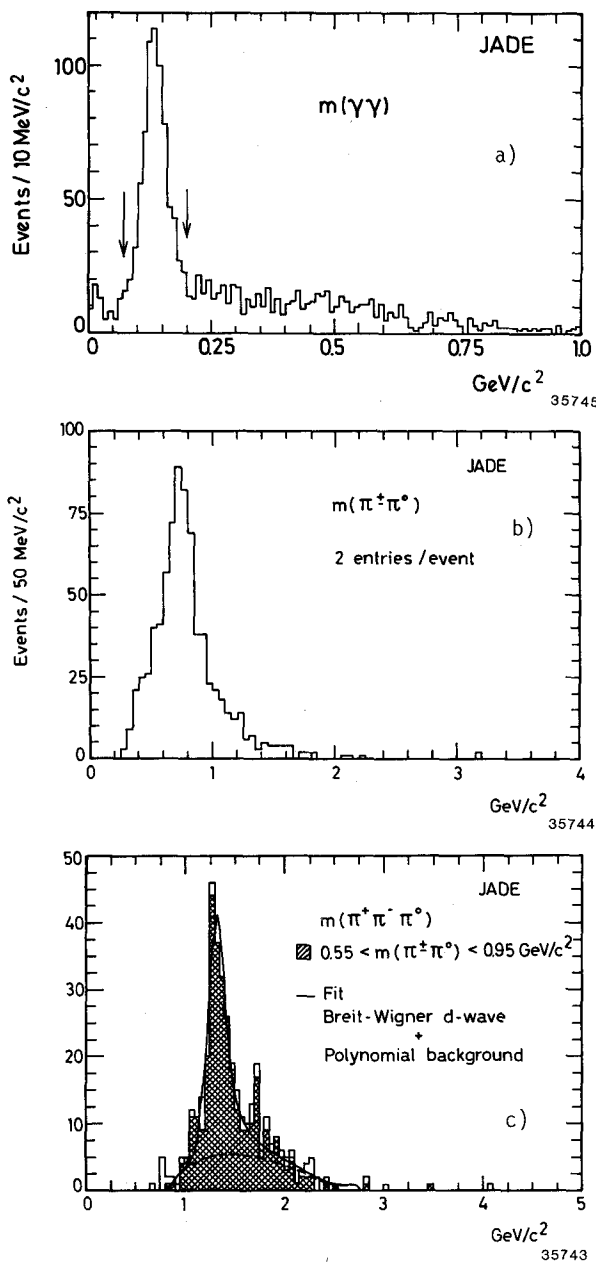


Fig. 10

- Mass of 2γ in exclusive $\pi^+\pi^-2\gamma$ events. The arrows indicate the π^0 band, 70-200 MeV/c^2 . Photon energies are > 90 MeV .
- Mass of $\pi^\pm\pi^0$ with two entries per event. Only those events from a) with $m(\gamma\gamma)$ combination in the π^0 band are included and $m(\gamma\gamma)$ is adjusted to the π^0 mass. A cut, $p_t(\pi^+\pi^-\pi^0) < 0.2$ GeV/c , has been applied.
- Mass of $\pi^+\pi^-\pi^0$ for the same events as in b). The shaded distribution contains events with at least one $\pi^+\pi^0$ mass combination in the ρ band.

the presence of another resonance state close to the f , which could give rise to interference effects. Production of $\epsilon(1300)$ however would give a different angular distribution of the π 's than the one observed and is probably small. A limit of $\Gamma_{\epsilon\gamma\gamma} \cdot B(\epsilon \rightarrow \gamma\gamma) < 1.5$ keV (95% C.L.) was set by the TASSO group⁽²²⁾. The mixing of the f with a nearby 2^{++} gluonium state has also been suggested⁽²⁸⁾; how to exclude or establish such a possibility is not clear.

The various measurements of $\Gamma_{f\gamma\gamma}$ are summarized in Table 2. The two values given for the Crystal Ball experiment correspond to the pure helicity 2 assumption and to the fit of different helicities to the $\pi^0\pi^0$ angular distribution. Only the former was used in calculating the weighted mean, $\Gamma_{f\gamma\gamma} = 2.8 \pm 0.2$ keV. The experimental values all fall in the lower end of the large range of values which have been predicted by various models^(29,34), ~ 1 keV to ~ 30 keV. Note here that many of the theoretical predictions are calculated with help of coupling constants determined from measurements of other decays; some of these measurements were grossly wrong, so that some predictions of $\Gamma_{f\gamma\gamma}$, if recalculated today, would change substantially.

$A_2(1320)$ production in $\gamma\gamma$ collisions was first seen by the Crystal Ball group, in the decay mode $A_2 \rightarrow \eta\pi^0 \rightarrow 4\gamma$. Last year the CELLO collaboration published⁽¹⁰⁾ a measurement of $\Gamma_{A_2\gamma\gamma}$, using the decay mode $A_2 \rightarrow \rho^\pm\pi^\mp \rightarrow \pi^+\pi^-\pi^0$. Only one of the photons from the π^0 was observed and the A_2 peak therefore appears in the same mass spectrum as η' , i.e. in the $\pi^+\pi^-\gamma$ spectrum (Fig. 4a). The JADE collaboration has made a complete reconstruction of the $2\pi^\pm\gamma$ final state and now presents data corresponding to an integrated luminosity of 77 pb^{-1} . The mass spectrum of the two photons is shown in Fig. 10a; it is dominated by the π^0 peak. Again, for events with a $\gamma\gamma$ mass combination in the π^0 mass band, the photon energies are adjusted so that the final state is $\pi^+\pi^-\pi^0$. The $\pi^\pm\pi^0$ mass is shown in Fig. 10b with a clear ρ^\pm signal. In fact, since there are two entries per event, almost all events are compatible with having a charged ρ . This is also obvious in Fig. 10c with the $\pi^+\pi^-\pi^0$ mass spectrum; the shaded distribution contains events with at least one $\pi^\pm\pi^0$ combination in the ρ band. The A_2 peak contains ~ 200 events. The value of the radiative width,

$$\Gamma_{A_2\gamma\gamma} = 0.84 \pm 0.07 \text{ (stat.)} \pm 0.15 \text{ (syst.) keV} \quad (\text{preliminary}),$$

is still preliminary, due to the not yet completed studies of the helicity structure of the reaction. The latter is studied with help of the angular distributions of the decay products. A preliminary result is 90% dominance of helicity 2, in good agreement with the findings for the f meson⁽²⁴⁾ and also with theoretical expectations for the tensor mesons⁽²⁹⁾. The value of $\Gamma_{A_2\gamma\gamma}$ was obtained with the assumption of pure helicity 2, like the previous two measurements.

The three measurements of $\Gamma_{A_2\gamma\gamma}$ are summarized in Table 2. The mean value is $\Gamma_{A_2\gamma\gamma} = 0.82 \pm 0.13$ keV. Theoretical predictions again span a wide range of values (29), from 0.3 keV to 30 keV, and the same remarks must be made as above for $\Gamma_{f\gamma\gamma}$. In SU(3), the ratio of $\Gamma_{A_2\gamma\gamma}$ to $\Gamma_{f\gamma\gamma}$ is a function of the tensor nonet mixing angle. Table 2 lists the values of the ratio $\Gamma_{A_2\gamma\gamma}/\Gamma_{f\gamma\gamma}$ for those groups which have measured both $\Gamma_{f\gamma\gamma}$ and $\Gamma_{A_2\gamma\gamma}$. The weighted mean is 0.32 ± 0.05 . Taking the ratio of the two mean values of $\Gamma_{A_2\gamma\gamma}$ and $\Gamma_{f\gamma\gamma}$ in Table 2, respectively, one obtains 0.30 ± 0.05 .

TABLE 2
Radiative Widths of Tensor Mesons

| Experiment | $\Gamma_{f\gamma\gamma} \pm (\text{stat.}) \pm (\text{syst.})$ keV |
|-----------------|--|
| PLUTO | $2.3 \pm 0.5 \pm 0.35$ |
| MARK II | $3.6 \pm 0.3 \pm 0.5$ |
| TASSO | $3.2 \pm 0.2 \pm 0.6$ |
| Crystal Ball | $2.7 \pm 0.2 \pm 0.6$ (helicity=2) |
| Crystal Ball | $2.9 \pm 0.6 \pm 0.6$ (helicity fit) |
| CELLO | $2.7 \pm 0.2 \pm 0.2$ (preliminary) |
| JADE | $2.3 \pm 0.2 \pm 0.5$ (preliminary) |
| Weighted Mean : | 2.8 ± 0.2 keV |

| Experiment | $\Gamma_{A_2\gamma\gamma} \pm (\text{stat.}) \pm (\text{syst.})$ keV |
|-----------------|--|
| Crystal Ball | $0.77 \pm 0.18 \pm 0.27$ |
| CELLO | $0.81 \pm 0.19 \pm 0.27$ |
| JADE | $0.84 \pm 0.07 \pm 0.15$ (preliminary) |
| Weighted Mean : | 0.82 ± 0.13 keV |

| Experiment | $\Gamma_{A_2\gamma\gamma}/\Gamma_{f\gamma\gamma}$ |
|-----------------|---|
| Crystal Ball | $0.29 \pm 0.07 \pm 0.07$ |
| CELLO | 0.30 ± 0.11 (preliminary) |
| JADE | 0.36 ± 0.08 (preliminary) |
| Weighted Mean : | 0.32 ± 0.05 |

The SU(3) prediction, given by eq.(10) and including the phase space factor $(m_{A_2}/m_f)^3$, is shown in Fig. 13a as function of the mixing angle θ . The two experimental ratios are shown as hatched bands. There is disagreement on the 1σ level with this simple SU(3) expectation and the experimental ratios do not limit the range of the mixing angle; however, one notes that the JADE value is in reasonable agreement

with the ideal mixing expectation (~ 0.40).

It should be commented here that normally the phase space factor is neglected in this ratio and the value 0.36 (9/25) is quoted as the SU(3) ideal mixing expectation.

The two photon production of the third neutral tensor meson, $f'(1515)$, was first observed by the TASSO collaboration⁽²⁷⁾ last year. It was seen in both decay modes, $f' \rightarrow K^+K^-$ and $f' \rightarrow \overset{\circ}{K} \overset{\circ}{K}$. In Fig. 11a the scatterplot of negative charge mass² vs. positive charge mass² is shown, as determined by TOF analysis in exclusive two prong events. The K^+K^- association is clearly seen. Fig. 11b shows the $\pi^+\pi^-$ mass (four combinations per event) from exclusive $4\pi^\pm$ events. A small $\overset{\circ}{K} \overset{\circ}{K}$ enhancement is visible. The shaded distribution shows the recoil $\pi^+\pi^-$ mass against those $\pi^+\pi^-$ combinations with a mass ($\pi^+\pi^-$) in a K^0 band. The associated $\overset{\circ}{K} \overset{\circ}{K}$ contribution is now obvious. The corresponding mass distributions of K^+K^- and $\overset{\circ}{K} \overset{\circ}{K}$ are given in Figs. 11a and b, respectively. Both spectra show an f' signal. In Fig. 11b, the $\pi\pi$ combinations have been constrained in a fit to the K^0 mass. In both samples the full statistics is used, 74 and 79 pb^{-1} , respectively. The analysis of these data samples is complicated by the fact that both f and A_2 decay into $K\bar{K}$ and they are close enough in mass to interfere with the f' . This interference is given by the following coherent sum(30),

$$\begin{aligned} \sigma_{\gamma\gamma \rightarrow K\bar{K}}(W_{\gamma\gamma}) &= 40\pi/W_{\gamma\gamma}^2 \cdot [|\Gamma_{f'\gamma\gamma} \cdot B(f' \rightarrow K\bar{K})|^{1/2} \cdot BW(f') \\ &\pm |\Gamma_{A_2\gamma\gamma} \cdot B(A_2 \rightarrow K\bar{K})|^{1/2} \cdot BW(A_2) \\ &+ |\Gamma_{f'\gamma\gamma} \cdot B(f' \rightarrow K\bar{K})|^{1/2} \cdot BW(f')]^2 \end{aligned}$$

where the different signs in the A_2 term refer to the different quark content in the two decay modes; the interference between A_2 and the isoscalars is destructive in the $\overset{\circ}{K} \overset{\circ}{K}$ decay.

The result of the analysis is shown in the fitted curves in Fig. 12a and b. The corresponding product of radiative width and branching ratio is

$$\Gamma_{f'\gamma\gamma} \cdot B(f' \rightarrow K\bar{K}) = 0.11 \pm 0.02 \text{ (stat.)} \pm 0.04 \text{ (syst.) keV}.$$

Pure helicity 2 was assumed for the production, in accordance with the experimental findings for f' ⁽²⁴⁾ and with theory⁽²⁹⁾. Helicity 0 contributions would make the above value larger, due to the difference in angular distribution in the decay of f' . Part of the large systematic error is due to the uncertainties in the A_2 and f contributions, which come from the measured values of $\Gamma_{f'\gamma\gamma}$ and $\Gamma_{A_2\gamma\gamma}$. This is also indicated in Fig. 12a.

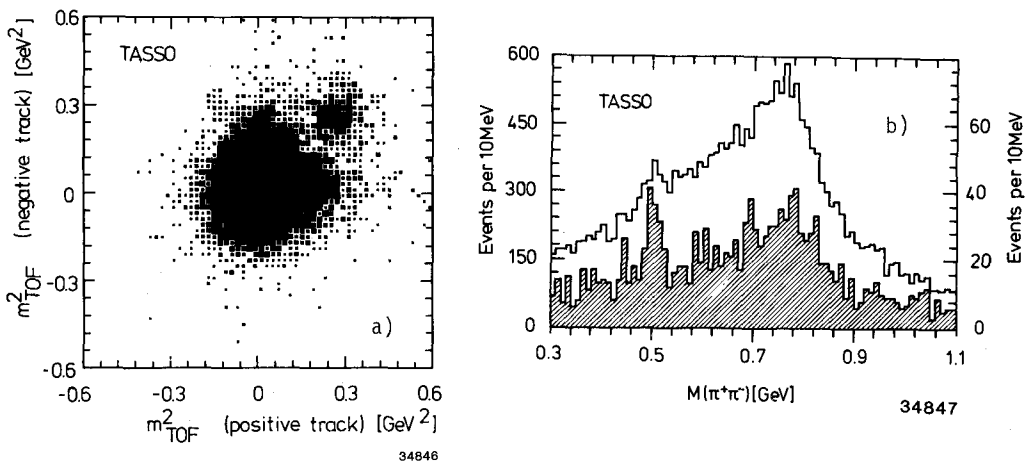


Fig. 11 a) Scatterplot of negative charge mass 2 vs. positive charge mass 2 for exclusive two prong events. The mass is determined by TOF analysis. b) Mass of $\pi^+\pi^-$, 4 combinations per event, in exclusive $4\pi^\pm$ events. The shaded distribution shows the $\pi^+\pi^-$ mass recoiling against a $\pi^+\pi^-$ combination within a K^0 band.

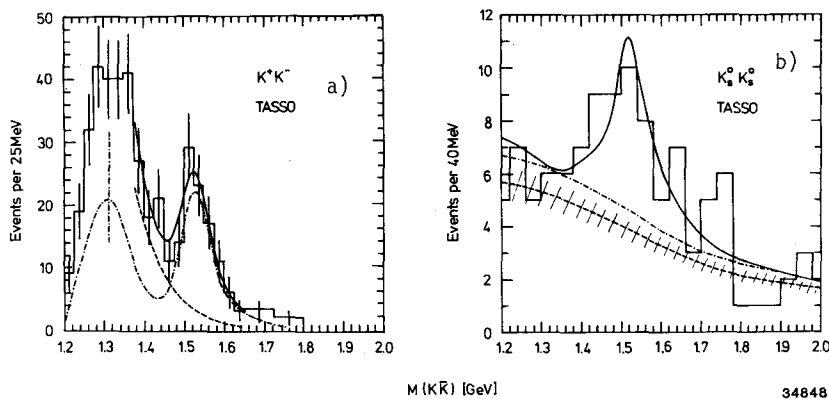


Fig. 12 a) Mass (K^+K^-) in exclusive K^+K^- events. A cut, $p_t(K^+K^-) < 0.15$ GeV/c, has been applied. The dashed curve shows the background in the fit and the dash-dotted curve the contribution from the interfering resonances f, A_2 and f' . The full curve shows the full fit. The error on the interference term is mainly due to uncertainties in $\Gamma_{A_2\gamma\gamma}$ and $\Gamma_{f\gamma\gamma}$. b) Mass ($K_S^0K_S^0$) in exclusive $4\pi^\pm$ events. A cut, $p_t(K_S^0K_S^0) < 0.15$ GeV/c, has been applied. The dashed curve shows the non $K_S^0K_S^0$ background and its uncertainty, the dash-dotted curve the full background, including the $K_S^0K_S^0$ part. The full curve shows the fit including the interference described in the text.

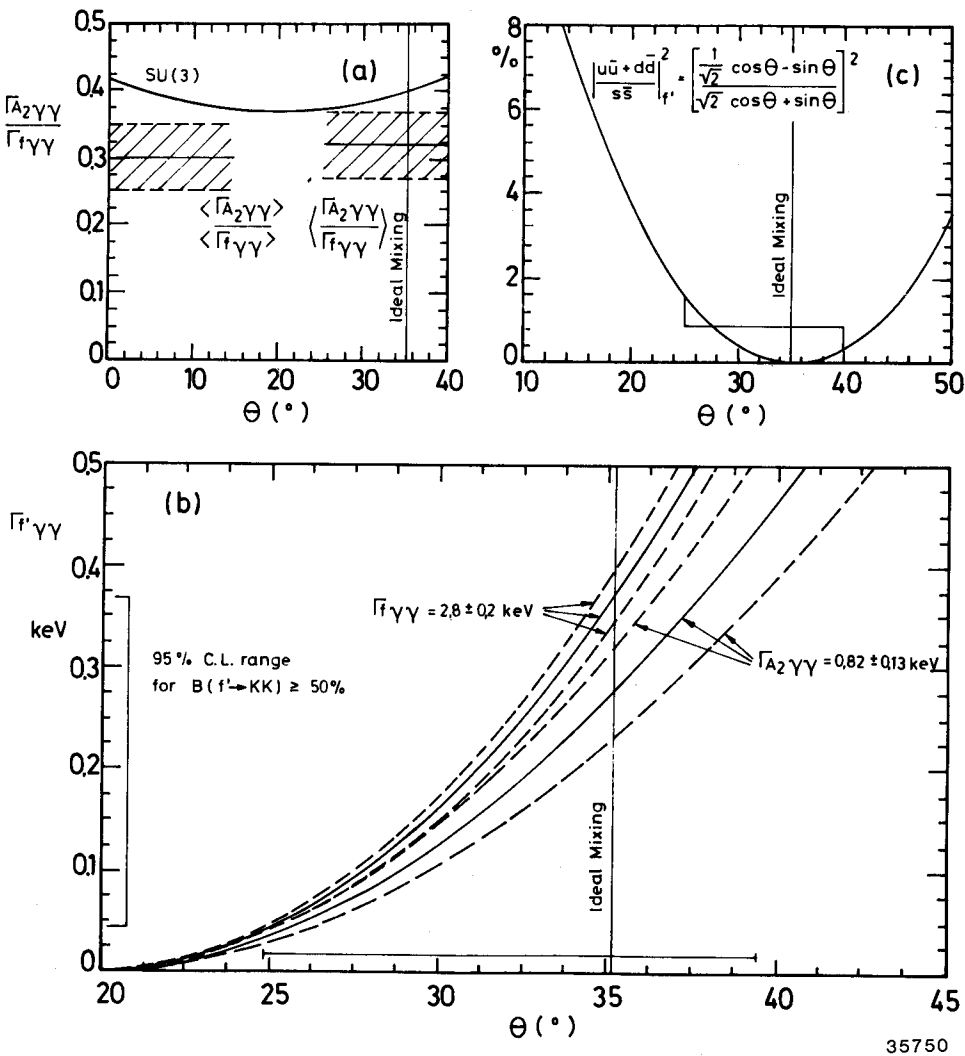


Fig. 13 a) The ratio $\frac{\Gamma_{A_2\gamma\gamma}}{\Gamma_{f'\gamma\gamma}}$ as function of mixing angle θ . The curve shows the SU(3) expectation, as given by eq.(10). The shaded bands are explained in the text. b) $\Gamma_{f'\gamma\gamma}$ as function of the mixing angle and the radiative widths $\Gamma_{A_2\gamma\gamma}$ and $\Gamma_{f'\gamma\gamma}$. The dependence on the latter is given by eq.(9). The two bands correspond to the weighted means in Table 2. The range in θ is given by the 95% C.L. range of $\Gamma_{f'\gamma\gamma}$ (the TASSO measurement and assuming $B(f' \rightarrow K\bar{K}) \geq 50\%$), through the intercepts with the f and A_2 bands. c) Percentage of non-strange quarks in f' , as function of the mixing angle θ . The intercept is the same range of θ as determined in Fig. 13b.

35750

Some of the theoretical work⁽²⁹⁾ for $\Gamma_{f\gamma\gamma}$ and $\Gamma_{A_2\gamma\gamma}$ also considers $\Gamma_{f'\gamma\gamma}$. Predictions range from 0.14 to 2.8 keV. In SU(3) the width $\Gamma_{f'\gamma\gamma}$ can be related to the mixing angle and to the other widths, $\Gamma_{A_2\gamma\gamma}$ and $\Gamma_{f\gamma\gamma}$. This is illustrated in Fig. 13b. Here the two curve bands correspond to the mean values of $\Gamma_{A_2\gamma\gamma}$ and $\Gamma_{f\gamma\gamma}$ from Table 2. Their non-overlapping is of course related to the situation in Fig. 13a; these values do not restrict the value of the mixing angle. It is interesting to note that for $\theta \approx 19.5^\circ$ the $\gamma\gamma$ width of f' vanishes, independent of the widths of f or A_2 . In Fig. 13b also the range in $\Gamma_{f'\gamma\gamma}$ is shown, corresponding to the TASSO measurement and to the assumption of $B(f' \rightarrow K\bar{K}) \geq 50\%$. The intercepts with the A_2 and f bands define a range in the mixing angle, $\sim 25^\circ < \theta < 40^\circ$. This range can be given a simple interpretation in terms of the content of non-strange quarks in f' . This content is clearly a function of the mixing angle and is shown in Fig. 13c. One sees that the present measurement restricts this content to at most a few %, also with less restrictive assumptions about $B(f' \rightarrow K\bar{K})$.

To finish this section on the tensor mesons, one may say that the $\gamma\gamma$ widths show reasonable agreement with the close to ideal mixing expected from studies of other reactions involving these resonances. There is still a large spread in the measurements of $\Gamma_{f\gamma\gamma}$ and a corresponding uncertainty in its ratio with the other $\gamma\gamma$ widths. More precise measurements of all these widths will be needed for more definite conclusions.

* * *

We come now to the last section of this review. No other states beyond the well known low mass pseudoscalar and tensor mesons have so far been seen in $\gamma\gamma$ collisions. Searches for in particular the scalar mesons (ϵ , S^* and δ), the charmed pseudoscalar η_c and the glueball candidates $\psi(1440)$ and $\theta(1640)$ have been carried out. The results, in form of upper limits, are summarized below.

The $\pi\pi$ spectrum from $\gamma\gamma$ collisions has a particular interest in such searches, since the two scalar mesons ϵ and S^* can be expected to show up here, both having major decay modes into $\pi\pi$. The $\pi^0\pi^0$ spectrum is the most sensitive place to look for such states, since it has no QED background to subtract, and a low level of $\pi^0\pi^0$ continuum. A limit for S^* production was set by the Crystal Ball group⁽²⁴⁾. At this conference the JADE group presents preliminary limits on the occurrence of narrow states between 0.55 and 1.0 GeV/c². These limits are derived from the mass spectrum in Fig. 9 and are shown as a curve in Fig. 14. Also shown is the S^* limit from the Crystal Ball group. Since the branching ratio $B(S^* \rightarrow \pi\pi)$ is now known, $78 \pm 3\%$ ⁽¹⁸⁾, the following limits on $\Gamma_{S^*\gamma\gamma}$ can be derived,

| | | |
|---------------------------------------|----------|--------------------|
| $\Gamma_{S^* \gamma\gamma} < 1.0$ keV | 95% C.L. | (Crystal Ball) |
| $\Gamma_{S^* \gamma\gamma} < 0.8$ keV | 95% C.L. | (JADE preliminary) |

The limits in Fig. 14 can be compared with the absence of narrow states in the radiative decay $J/\psi \rightarrow \gamma\pi^0\pi^0$ ⁽³¹⁾. In the latter process narrow ($\Gamma < 100$ MeV) states with masses between 500 and 1000 MeV were searched for and a limit, $B(J/\psi \rightarrow \gamma X \rightarrow \gamma\pi^0\pi^0) < 1.3 \cdot 10^{-5}$, 95% C.L., was placed on their occurrence. In contrast, the known radiative decays of J/ψ generally have branching ratios of the order 10^{-3} ⁽¹⁸⁾. For further discussion, see Ref. 31.

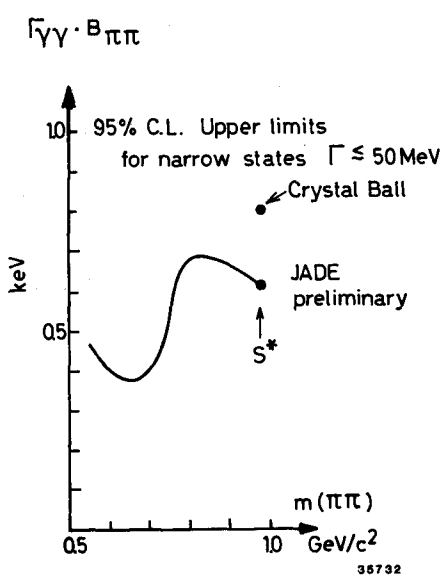


Fig. 14

95% C.L. limit on the product of $\Gamma_{\gamma\gamma} \cdot B_{\pi\pi}$, as function of the mass of the resonance R . The width of R is $\lesssim 50$ MeV and $B_{\pi\pi}$ is the branching ratio into $\pi\pi$

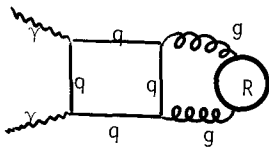
Limits on the production of broad (i.e. with widths \gtrsim a few hundred MeV) states below $1 \text{ GeV}/c^2$ in $\gamma\gamma$ reactions are not yet available. They would be of interest for the question of ϵ (or σ) production, e.g. in the DML experiment⁽³²⁾ at DCI, a broad low mass ϵ is invoked to explain the excess of $\pi^+\pi^-$ events above the expectation from the Born term calculation. For further discussion of $\gamma\gamma$ production of scalar states, see Refs. 16, 24, 26, 33 and 34.

The few events around $2 \text{ GeV}/c^2$ in Fig. 9 have been used by the JADE group to obtain a limit on $\gamma\gamma$ production of the $h(2040)$ meson. This limit is given as

$$\Gamma_{h\gamma\gamma} \cdot B(h \rightarrow \pi\pi) < 0.22 \text{ keV} \quad 95\% \text{ C.L.} \quad (\text{preliminary})$$

corresponding to $\sigma(e^+e^- \rightarrow e^+e^-h) \cdot B(h \rightarrow \pi\pi) \lesssim 60 \text{ pb}$. Here isotropic decay of the h meson was assumed. In Ref. 34 $\sigma(e^+e^- \rightarrow e^+e^-f^*)$, f^* being the f recurrence, is estimated to $\sim 0.4 \text{ nb}$.

The production of glueballs in $\gamma\gamma$ production is naively expected to be suppressed, compared with $q\bar{q}$ meson production. This is because the photons do not couple directly to the gluons, but only via an intermediate quark loop,



Since an extra quark loop is involved, one could expect an order of magnitude suppression, corresponding to the square root of the Okubo-Zweig-Iizuka-factor⁽³⁵⁾, $\sqrt{\text{OZI}} \sim 10$. This

is at the limit of present statistics at PETRA and PEP. Nevertheless, glueballs have been searched for in $\gamma\gamma$ collisions. Of particular interest are the states $\psi(1440)$ and $\Theta(1640)$, which have been seen in radiative J/ψ decays⁽³⁶⁾ and which have no natural place in the $SU(3)$ nonets. Since J/ψ radiative decays are a likely source of glueball production⁽³⁷⁾, both ψ and Θ are now counted as candidates for such states. A number of models have been put forth that mix these states with the iso-scalar members of the pseudoscalar and tensor nonets⁽³⁸⁾. In such models, gluonium states may acquire larger $\gamma\gamma$ widths due to the mixing with $q\bar{q}$ states. Definite predictions may be made about decay modes for all the involved states, and also for widths of the decays into $\gamma\gamma$. Thus the results of the experimental searches are important, although presently only upper limits are given.

TABLE 3
Upper limits for $\gamma\gamma$ widths of ψ and Θ

| Experiment ^(Ref.) | Decay Mode X | $\Gamma_{\psi\gamma\gamma} \cdot B(\psi \rightarrow X)$ | 95% C.L. |
|------------------------------|----------------|---|----------|
| MARK II ⁽⁹⁾ | $K\bar{K}\pi$ | < 8.0 keV | |
| TASSO ⁽³⁹⁾ | $K\bar{K}\pi$ | < 7.0 keV (preliminary) | |
| TASSO ⁽⁴⁰⁾ | $\rho^0\rho^0$ | < 1.0 keV | |

| Experiment ^(Ref.) | Decay Mode X | $\Gamma_{\Theta\gamma\gamma} \cdot B(\Theta \rightarrow X)$ | 95% C.L. |
|------------------------------|----------------|---|----------|
| Crystal Ball ⁽³¹⁾ | $\eta\eta$ | < 0.3 keV | |
| MARK II ⁽⁴¹⁾ | $K\bar{K}$ | < 0.4 keV | |
| TASSO ⁽³⁹⁾ | $K\bar{K}$ | < 0.3 keV (preliminary) | |
| TASSO ⁽⁴⁰⁾ | $\rho^0\rho^0$ | < 1.2 keV | |

Several decay modes of ψ and Θ have been investigated and the present limits are summarized in Table 3. Some of the data underlying these limits are shown in the talks by H. Spitzer and H. Kolanoski, these proceedings.

$K\bar{K}\pi$ is so far the only decay mode of ψ which has been seen. If it indeed is the major decay mode, i.e. $B(\psi \rightarrow K\bar{K}\pi) \gtrsim 50\%$, then $\Gamma_{\psi\gamma\gamma} \lesssim 15$ keV. This is not yet restrictive although some models do predict a $\gamma\gamma$ width in this range. The limit involving $B(\psi \rightarrow \rho^0\rho^0)$ contradicts the large estimate in the model by Milton, Palmer and Pinski⁽³⁸⁾. For Θ , the only known decay modes are $\eta\eta$ and $K\bar{K}$. A possible third decay mode is $\Theta \rightarrow \rho^0\rho^0$. Recently a resonance like enhancement in the radiative decay $J/\psi \rightarrow \gamma\rho^0\rho^0$,

with the branching ratio $(1.25 \pm 0.35 \pm 0.40) \cdot 10^{-3}$, was reported⁽⁴²⁾. If interpreted as a Breit-Wigner resonance, the mass and width of this state are very similar to those of $\Theta(1640)$. If these decay modes dominate, then the limits in Table 3 places limits on $\Gamma_{\Theta\gamma\gamma}$ that are in the same range as current predictions, $\lesssim 1$ keV.

The $\gamma\gamma$ production of $\eta_c(2980)$ is heavily suppressed due to the large mass, since the cross section is proportional to $m_{\eta_c}^{-3}$, cfr. eq.(5). However, theoretical estimates⁽⁴³⁾ give η_c a rather large $\gamma\gamma$ width, ~ 6 keV. This corresponds at PETRA and PEP beam energies to $\sigma(e^+e^- \rightarrow e^+e^-\eta_c) \sim 50$ pb and thus to ~ 4000 events presently at each PETRA interaction point. Small detection efficiencies and the smallness of the known decay modes of η_c again puts it at the limit of detection with the present statistics. The theoretical estimates are based on two different approaches : in the non-relativistic potential models⁽⁴³⁾,

$$\Gamma_{\eta_c\gamma\gamma} = \frac{12\alpha^2 Q_c^4 |R_s(0)|^2}{m_{\eta_c}^2} \quad \Gamma_{J/\Psi e^+e^-} = \frac{4\alpha^2 Q_c^2 |R_s(0)|^2}{m_{J/\Psi}^2}$$

where $R_s(0)$ is the s-wave radial wave function at the origin and Q_c the charm quark charge. Since the mass difference of η_c and J/Ψ is small, the assumption that the two wave functions are equal is made and

$$\Gamma_{\eta_c\gamma\gamma} = \frac{4}{3} \Gamma_{J/\Psi e^+e^-} \quad \text{or} \quad \Gamma_{\eta_c\gamma\gamma} \approx 6 \text{ keV}.$$

More careful considerations of the difference in $R_s(0)$ modify this estimate to 5.5 keV. Similar estimates are obtained with the QCD based dispersion sum rule calculations^(43,44), in the range 4 - 7 keV. In view of the success with which the sum rule calculations have been applied to the charmonium system, a precise measurement of $\Gamma_{\eta_c\gamma\gamma}$, as well as the $\gamma\gamma$ widths of the heavier charmonium states $\chi_0(3415)$, $\chi_2(3555)$ and $\eta_c'(3590)$, will be an important test. The measurement of $\Gamma_{\eta_c\gamma\gamma}$ is therefore of great interest and almost all known decay modes of η_c ⁽⁴⁵⁾ have been used for the searches. The results are summarized in Table 4. To give an idea of the present experimental sensitivity, Fig. 15 shows the $4\pi^\pm$ spectrum from the TASSO group, together with the gaussian fit which gives the present limit in this decay mode. Similarly the JADE data in Fig. 16 shows the $2\pi^+2\pi^0$ spectrum. Here all events in the η_c region were used to set the upper limit. One may conclude from Table 4 that both more data and better known decay modes of η_c are needed for the eventual measurement of $\Gamma_{\eta_c\gamma\gamma}$. The experimental limits, together with the poorly known branching ratios of η_c , give corresponding limits on $\Gamma_{\eta_c\gamma\gamma}$ of the order of 50-100 keV or more. The lowest limit so far is obtained by the Crystal Ball group⁽⁴⁷⁾, from the decay $J/\Psi \rightarrow 3\gamma$: $\Gamma_{\eta_c\gamma\gamma} \lesssim 20$ keV, which is still well above the theoretical predictions.

It should be mentioned here that the decay $\chi_2(3555) \rightarrow \gamma\gamma$ has been observed by the

Crystal Ball group in the reaction $\psi' \rightarrow 3\gamma$ ⁽⁴⁶⁾. The reported values for the branching ratio, $B(\chi_2 \rightarrow \gamma\gamma) = (6 \pm 2) \cdot 10^{-4}$, and absolute width of $\chi_2(3555)$, $\Gamma_X = 2.1 + 1.0 - 0.7$ MeV⁽⁴⁶⁾, correspond to a value $\Gamma_{\chi_2} = 1.3 + 0.7 - 0.6$ keV. From the dispersion sum rule calculations the estimate $1.7 - 2.3$ keV is given (Novikov et al. (43)). Similarly, for $\chi_0(3415)$ a limit can be obtained, $\Gamma_{\chi_0} < 9.2$ keV (90% C.L.). Here the values $4.6 - 5.4$ keV have been predicted (Novikov et al. (43)).

Table 4
Upper Limits for $\gamma\gamma$ Production of η_c

| Experiment (Ref) | Decay Mode X | $\Gamma_{\eta_c \rightarrow \gamma\gamma}$ keV preliminary | $B(\eta_c \rightarrow X)$ (45, 46) % |
|-----------------------|----------------------|---|--|
| TASSO ⁽³⁹⁾ | $p\bar{p}$ | < 0.4 | 95% C.L. |
| TASSO ⁽³⁹⁾ | $K\bar{K}\pi$ | < 27 | 95% C.L. |
| TASSO ⁽³⁹⁾ | $2\pi^+ 2\pi^-$ | < 0.7 | 95% C.L. |
| JADE ⁽³⁹⁾ | $\pi^+ \pi^- 2\pi^0$ | < 4.2 | 95% C.L. |
| JADE ⁽³⁹⁾ | $\eta\pi^+ \pi^-$ | < 2.3 | 95% C.L. |

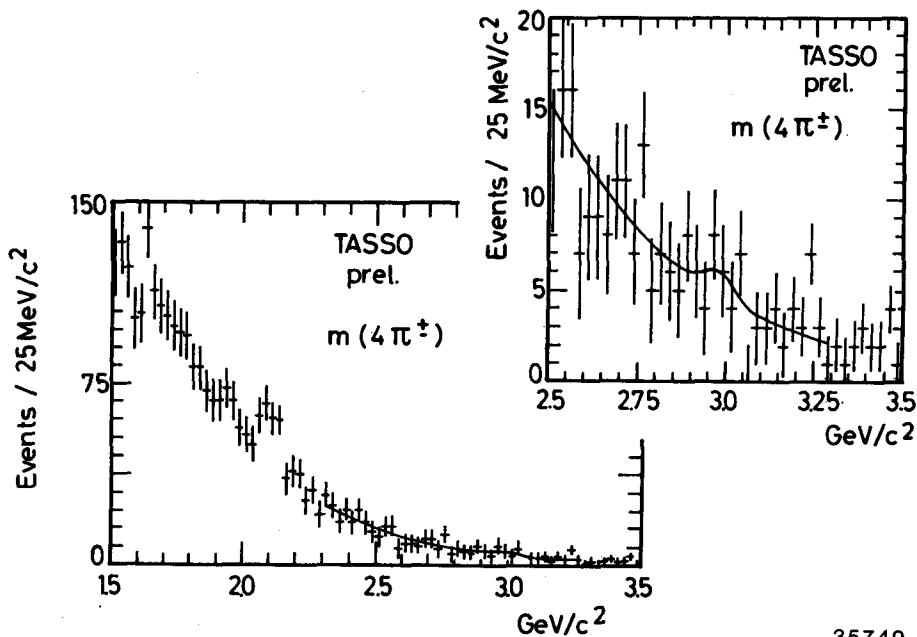


Fig. 15 Mass spectrum of $4\pi^\pm$ in exclusive $4\pi^\pm$ events. The insert shows the same data in magnified scale. The fit is a smooth background with a gaussian resolution function corresponding to the known $4\pi^\pm$ mass resolution at the η_c mass.

Although the above results are still meager, it is clear that future larger data samples will provide important information on these radiative widths. Continued studies of the charmonium states and their decays, at the J/ψ and ψ' resonances, will be as important in this respect.

This review closes with an example of the possibility to use the large integrated luminosities for the study of rare decay modes of well known $C = +1$ resonances. The JADE group presents at this conference a search for the decay $f \rightarrow \pi^+ \pi^- 2\pi^0$. While the corresponding all charged decay $f \rightarrow 4\pi^\pm$ is well known, $2.8 \pm 0.4\%$ ⁽¹⁸⁾, the partly neutral decay is poorly known. Expected is $B(f \rightarrow \pi^+ \pi^- 2\pi^0) = (1-2) \cdot B(f \rightarrow 4\pi^\pm)$, depending on the isospin structure of the decay. The data are shown in Fig. 16. In these data, no background subtraction (from π^0 sidebands) has yet been done and the word preliminary should be stressed. A more detailed presentation of these data, in particular concerning the presence of a $\rho^+ \rho^-$ component, is given by H. Kolanoski elsewhere in these proceedings. In Fig. 15, events which are candidates for the process $\gamma\gamma \rightarrow \rho^+ \rho^-$ have been removed and the decay $f \rightarrow \rho^+ \rho^-$ is not considered. All events below $1.6 \text{ GeV}/c^2$ are taken as candidates for the f decay. The rate is compared with the rate of $e^+ e^- \rightarrow e^+ e^- f \rightarrow e^+ e^- \pi^0 \pi^0$, which was observed in the same experiment, and this gives the limits

$$B(f \rightarrow \pi^+ \pi^- 2\pi^0) < 0.12 \quad 95\% \text{ C.L. (preliminary)}$$

$$B(f \rightarrow \pi^+ \pi^- 2\pi^0) / (B(f \rightarrow \pi\pi)) < 0.15 \quad 95\% \text{ C.L. (preliminary)}.$$

The latter value can be compared with the previous measurement ⁽⁴⁸⁾, $15 \pm 7\%$.

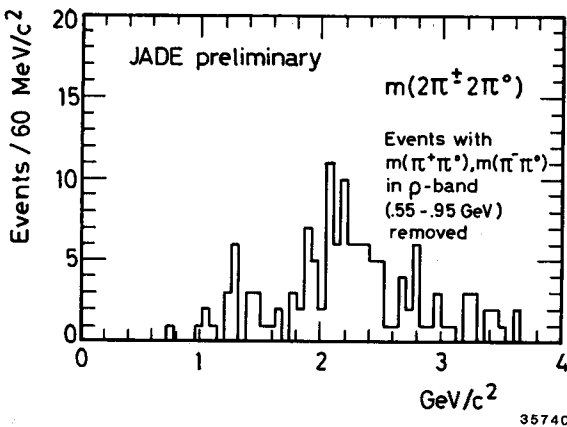


Fig. 16 Mass of $2\pi^\pm 2\pi^0$ in exclusive $\pi^+ \pi^- 4\gamma$ events. All events with two $\pi^\pm \pi^0$ combinations in ρ bands have been removed. The $\gamma\gamma$ combinations in a π^0 band were adjusted to the π^0 mass. A cut, $p_t(2\pi^\pm 2\pi^0) < 0.2 \text{ GeV}/c$, has been applied. The data correspond to 77 pb^{-1} .

CONCLUSIONS

Resonance production in $\gamma\gamma$ reactions continues to provide much useful information to test our ideas about the quark structure of mesons. Large amounts of data have already been collected at SPEAR, PETRA and PEP and these data are being analyzed. To resolve questions about the $\gamma\gamma$ couplings of scalars, glueballs and heavy mesons like η_c , much higher statistics is needed. This will take some time to come, at least at PETRA, since present plans foresee running at highest possible energies, with corresponding lower luminosities. Much work however remains to be done with the existing data, not only in investigating new exclusive final states but also in the better understanding of the detectors and of the physics involved.

Acknowledgement

I wish to thank all my colleagues at DESY and SLAC for giving freely of their time and knowledge and for providing the material for this review. Thanks are also due to the organizers of this workshop, for providing such nice surroundings for a successful meeting.

REFERENCES

1. G. Bellettini et al.,
V.I. Kryshkin et al.,
A. Browman et al.,
Nuovo Cim. 66A (1970) 243
JETP 30 (1970) 1037
Phys.Rev.Lett. 33 (1974) 1400
2. C. Bemporad et al.,
A. Browman et al.,
Phys.Lett. 25B (1967) 380
Phys.Rev.Lett. 32 (1974) 1067
3. C.N. Yang,
Phys.Rev. 77 (1950) 242
4. G. Bonneau, M. Gourdin and F. Martin, Nucl. Phys. B54 (1973) 573
J. Field,
Nucl.Phys. B168 (1980) 477,
and Erratum Nucl.Phys.B176 (1980) 545
5. R.B. Curtis,
R.H. Dalitz and D.R. Yenni,
Phys.Rev. 104 (1956) 211
Phys.Rev. 105 (1957) 1598
6. F.E. Low,
Phys.Rev. 120 (1960) 582
7. I.F. Ginzburg and V.G. Serbo, Phys.Lett. 109B (1982) 231
8. A. Rittenberg,
UCRL-18863 (1969), Thesis, unpublished
9. MARK II Coll., G. Abrams et al., Phys.Rev.Lett. 43 (1979) 477
MARK II Coll., P. Jenni et al., Phys.Rev. D27 (1983) 1031
10. CELLO Coll., H.J. Behrend et al., Phys.Lett. 114B (1982) 378,
and Erratum, Phys.Lett. 125B (1983) 518
11. JADE Coll., W. Bartel et al., Phys.Lett. 113B (1982) 190
12. F. Close,
An Introduction to Quarks and Partons
(Academic Press, London, 1979).
13. G. von Dardel et al.,
G. Bellettini et al.,
Phys.Lett. 4 (1963) 51
Nuovo Cim. 40A (1965) 1139.
14. CERN/SPSC/82-35 and CERN/SPSC/82-40 (Proposal)

15. PLUTO Coll., presented by M. Zachara in the parallel sessions, see H. Spitzer, these proceedings.

16. S. Matsuda and S. Oneda, Phys.Rev. 187 (1969) 2107
S. Okubo, in *Symmetries and Quark Models*, ed. R. Chand (Gordon and Breach, New York, 1970)

H. Suura, T.F. Walsh and B.-L. Young, Lett. Nuovo Cim. 4 (1972) 505
A. Bramon and M. Greco, Phys.Lett. 48B (1974) 137
F. Gault et al., Nuovo Cim. 24A (1974) 259
A. Kazi, G. Kramer and D.H. Schiller, Lett. Nuovo Cim. 15 (1976) 120
N. Isgur, Phys.Rev. D13 (1976) 129
Etim-Etim and M. Greco, Nuovo Cim. 42 (1977) 124
V.M. Budnev and A.E. Kaloshin, Phys.Lett. 86B (1979) 351
M. Chanowitz, Phys.Rev.Lett. 35 (1979) 977
ibid., Phys.Rev.Lett. 44 (1980) 59

17. D. Binnie et al., Phys.Lett. 83B (1979) 141

18. Particle Data Group, Phys.Lett. 111B (1982) 1

19. A.T. Filippov, Sov. J. Nucl.Phys. 29 (1979) 534

20. W.D. Apel et al., Sov. J. Nucl.Phys. 25 (1977) 300

21. M. Chanowitz, Proc. SLAC Summer Institute on Particle Physics, 1981

22. PLUTO Coll., Ch. Berger et al., Phys.Lett. 94B (1980) 254
TASSO Coll., R. Brandelik et al., Z. Phys. C10 (1981) 117

23. MARK II Coll., A. Roussarie et al., Phys.Lett. 105B (1981) 304

24. Crystal Ball Coll., C. Edwards et al., Phys.Lett. 110B (1982) 82

25. PLUTO Coll., Ch. Berger et al., Nucl.Phys. B202 (1982) 189

26. G. Mennessier, Z. Phys. C16 (1982) 241

27. TASSO Coll., M. Althoff et al., Phys.Lett. 121B (1983) 216

28. J.L. Rosner, Phys.Rev. D24 (1981) 1347
J.F. Donoghue, Phys.Rev. D25 (1982) 1875

29. A rather complete list is found in
PLUTO Coll., Ch. Berger et al., Phys.Lett. 94B (1980) 254
In addition, and of newer date are, e.g.
G.M. Radutskii, JETP Lett. 6 (1967) 336
Z. Kunszt, R.M. Muradyan and V.M. Ter-Atonyan, Budna Report E2-5424 (1970)
D. Faiman, H.J. Lipkin and H.R. Rubinstein, Phys.Lett. 59B (1975) 269
P. Grassberger and R. Kögerler, Nucl.Phys. B106 (1976) 451
H. Krasemann and J.A.M. Vermaseren, Nucl. Phys. B184 (1981) 269
P. Singer, Phys.Lett. 124B (1983) 531
L. Bergström, G. Hulth and H. Snellman, Z. Phys. C16 (1983) 263

30. H.J. Lipkin, Nucl.Phys. B7 (1968) 321
ibid., Proc. EPS Int. Conf. on High Energy Physics, Palermo 1975, p. 609
D. Faiman et al., Ref. 29

31. K. Wacker, Proc. of the XVIIth Rencontre de Moriond, La Plagne, March 13-19, 1983

32. A. Coureau et al., Phys.Lett. 96B (1980) 402
A. Falvard et al., Paper No. 48 submitted to the Int. Symposium on Lepton and Photon Interactions at High Energies, Bonn 1981

33. V.M. Budnev, A.N. Vall and V.V. Serebryakov, Sov. J. Nucl.Phys. 21 (1975) 531
 A.E. Kaloshin and V.V. Serebryakov, Iph-125, Novosibirsk 1981
 D.H. Lyth, University of Lancaster preprint May 1982

34. B. Schrempp-Otto, F. Schrempp and T.F. Walsh, Phys.Lett. 36B (1971) 463
 and private communication

35. S. Okubo, Phys.Lett. 5 (1963) 105
 G. Zweig, CERN Report 8182/TH.401 (1964)
 J. Iizuka et al., Prog. Theor. Phys. 35 (1966) 1061

36. Crystal Ball Coll., C. Edwards et al., Phys.Rev.Lett.49 (1982) 259
 and Erratum, Phys.Rev.Lett. 50 (1983) 219
 ibid., Phys.Rev. Lett. 48 (1982) 458

37. J.D. Bjorken, Proc. Int. Conf. on High Energy Physics, Geneva 1979, p.245
 S. Meshkov, Proc. Orbis Scientiae, Coral Gables, 1980, p.43
 M. Chanowitz, Proc. SLAC Summer Institute, Stanford, 1981

38. C. Rosenzweig, A. Salomone and J. Schechter, Phys.Rev. D24 (1981) 2545
 S. Iwao, Lett. Nuovo Cim. 35 (1982) 481
 J.F. Donoghue, Proc. XVIth Int. Conf. on High Energy Physics, Paris, 1982, p. C3-89
 K. Senba and M. Tanimoto, Phys.Rev. D25 (1982) 792
 ibid., Phys.Rev. D26 (1982) 3270
 T. Teshima and S. Oneda, Phys.Lett. 123B (1983) 455
 ibid., Phys.Rev. D27 (1983) 1551
 S. Ono and O. Pène, Phys.Lett. 109B (1982) 101
 K.A. Milton, W.F. Palmer and S.S. Pinsky, Proc. of the XVIIth Rencontre de Moriond, Les Arcs, France, March 20-26, 1982
 W.F. Palmer and S.S. Pinsky, Phys.Rev. D27 (1983) 2219
 J. Schechter, Phys.Rev. D27 (1983) 1109
 B. Li et al., Beijing Institute of High Energy Physics, preprint, BIHEP Th-82-10, June 1982
 J.L. Rosner, Phys.Rev. D24 (1981) 1347
 ibid., Phys.Rev. D27 (1983) 1101
 J.L. Rosner and S.F. Tuan, Phys.Rev. D27 (1983) 1544
 E. Kawai, Phys.Lett. 124B (1983) 262
 J.F. Donoghue and H. Gomm, Phys.Lett. 121B (1983) 49
 S.-C. Chao, University of Oregon preprint, OITS 205, Dec. 1982
 N. Aizawa, Z. Maki and I. Umemura, Kyoto University preprint, July 1982

39. TASSO and JADE Collaborations, data submitted to this conference

40. TASSO Coll., M. Althoff et al., Z. Phys. C16 (1982) 13

41. D.L. Burke, Proc. XVIth Int. Conf. on High Energy Physics, Paris, 1982, p. C3-513

42. MARK II Coll., D.L. Burke et al., Phys.Rev.Lett. 49 (1982) 632

43. V.A. Novikov et al., Phys.Reports 41C (1978) 1
 T. Appelquist, R.M. Barnell and K.D. Lane, Ann.Rev.Nucl.Part.Sci. 28 (1978) 387
 M.A. Shifman, Z.Phys. C4 (1980) 345
 L. Bergström, H. Snellman and G. Tengstrand, Phys.Lett. 82B (1979) 419

44. V.A. Novikov et al., Phys.Rev.Lett. 38 (1977) 626
 ibid., Phys.Lett. 67B (1977) 409
 R. Kirschner and A. Schiller, Z. Phys. C16 (1982) 141
 L.J. Reinders, H.R. Rubinstei and S. Yazaki, Phys.Lett. 113B (1982) 411

45. MARK II Coll., T.M. Himmel et al., Phys.Rev.Lett. 45 (1980) 1146
 Crystal Ball Coll., R. Partridge et al., Phys.Rev.Lett. 45 (1980) 1150

46. M. Oreglia, Proc. of the XVth Rencontre de Moriond, Les Arcs, France, March 15-21, 1980
 J.E. Gaiser, Proc. of the XVIIth Rencontre de Moriond, Les Arcs, France, Jan.24-30, 1982

E. Bloom, Proc. "Physics in Collision", Stockholm, 1982

47. K. Königsmann, Proc. XVIIth Rencontre de Moriond, Les Arcs, France, March 14-20, 1982

48. Y. Eisenberg et al., Phys.Lett. 52B (1974) 239.

Discussion

Q. P. SINGER (Haifa) : Concerning the new result for $\pi \rightarrow \gamma\gamma$, I wonder what happened with the very first measurement of Bemporad et al., which gave a value close to 1 keV? It seems that the Crystal Ball value comes inbetween the old DESY value and the Cornell value.

A. OLSSON : Browman et al. (Cornell 1974) state in their paper that their fit coefficients are compatible with the DESY data from 1967 (Bemporad et al.), although the sets of coefficients are different in the two experiments. They suggest that the DESY data may not be sensitive enough to distinguish the two solutions, mainly due to limited energy range. The DESY measurement is not included by PDG in a mean value for $\Gamma_{\pi\gamma\gamma}$.

Q. J.A.M. VERMASEREN (NIKHEF) : What is known about the f in the tagged data ?

A. OLSSON : The TASSO group showed data on tagged f production in Paris 1981, but no signal could be claimed. No data were submitted to this review talk, although the PLUTO group will show some results in the parallel sessions. Again, no signal is seen.

VERMASEREN : This shows also that the form factors are very strong.

Q. S. BRODSKY (SLAC) : I don't believe it is appropriate to use a unitarized Born-term model based on point-like pions and kaons to estimate the background to resonance production in $\gamma\gamma\pi^+\pi^-$ and $\gamma\gamma K^+K^-$. The fall-off of the meson form factors should give an index of the expected suppression of the continuum contribution due to meson compositeness.

A. OLSSON : Experimentalists are of course happy to have at least one model that seems to explain the data, including the mass shift of the f meson and the large low mass continuum. But for the details of your question I must refer you to Mennessier.

G. MENNESSIER (Montpellier) : To describe the nearby left hand cut, one needs Born terms. Notice that because of gauge invariance, one cannot introduce a true form factor for the pion (or kaon) exchange. Of course farther singularities are expected to become more important with higher energies and should be included. Several exchanges have been tried, with or without form factors. It turns out that a correct description of the data up to the f mass can be achieved with the pure point-like Born term.

I agree that a model for the t and u channel singularities which would interpolate between the Born behaviour at low energies and the scaling behaviour expected at high energies would be more satisfactory from a theoretical point of view. It does not seem necessary within the present status of experimental data.